

# Nitroxide-Mediated Controlled Free-Radical Emulsion Polymerization Using a Difunctional Water-Soluble Alkoxyamine Initiator. Toward the Control of Particle Size, Particle Size Distribution, and the Synthesis of Triblock Copolymers

Julien Nicolas,<sup>†</sup> Bernadette Charleux,<sup>\*,†</sup> Olivier Guerret,<sup>‡</sup> and Stéphanie Magnet<sup>‡</sup>

Laboratoire de Chimie Macromoléculaire, UMR CNRS-UPMC 7610, Université Pierre et Marie Curie, T44, E1, 4, Place Jussieu, 75252 Paris Cedex 05, France, and ARKEMA, Groupement de Recherches de Lacq, B.P. No. 34, 64170 LACQ, France

Received June 8, 2005; Revised Manuscript Received September 16, 2005

**ABSTRACT:** A novel dialkoxyamine bearing two carboxylic acid groups was synthesized by the addition of a high dissociation rate constant alkoxyamine onto tri(ethylene glycol) diacrylate. This dialkoxyamine was first successfully used as an initiator for the bulk polymerizations of *n*-butyl acrylate and styrene. Then the sodium salt counterpart was used as a water-soluble initiator in the emulsion polymerizations of *n*-butyl acrylate and styrene via a multistep process. Owing to its unique structure with two carboxylate salts remaining covalently bound to the chain and hence locked at the particle surface, very stable latexes were recovered with, for the first time, small particles and narrow particle size distributions. The emulsion process was successfully applied to the synthesis of well-defined poly(*n*-butyl acrylate) and polystyrene homopolymers as well as polystyrene-*b*-poly(*n*-butyl acrylate)-*b*-polystyrene triblock copolymer. This work represents the first successful attempt of the synthesis of a complex architecture together with the control of average diameter and particle size distribution in nitroxide-mediated polymerization in emulsion, which is of high industrial and academic interest.

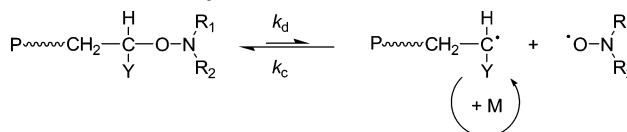
## Introduction

Nitroxide-mediated controlled-free radical polymerization (NMP) represents one of the most advantageous methods for synthesizing tailor-made macromolecular architectures.<sup>1–3</sup> Indeed, the controlled free-radical polymerization methods, including also atom transfer radical polymerization (ATRP)<sup>4,5</sup> and reversible chain transfer (i.e., iodine transfer polymerization,<sup>6,7</sup> reversible addition–fragmentation chain transfer,<sup>8–10</sup> and organotellurium-mediated polymerization<sup>11</sup>), combine the advantages of both the ionic polymerizations in term of livingness and the free radical polymerization in term of process implementation.<sup>12–14</sup>

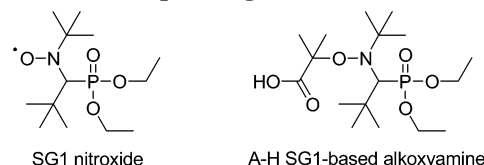
NMP is based on a reversible activation–deactivation equilibrium (Scheme 1) in which the nitroxide reversibly deactivates the growing radical into an alkoxyamine dormant end-functionality. The activation reaction is a thermal process, which represents a significant advantage since neither metallic catalyst nor bimolecular exchange between macromolecular species is required. Compared to TEMPO (2,2,6,6-tetramethylpiperidinyl-1-oxy) and its derivatives, which are well-suited for styrenic monomers only, the second generation of nitroxides<sup>15,16</sup> such as SG1 (*N*-*tert*-butyl-*N*-(1-diethylphosphono-2,2-dimethylpropyl)-*N*-oxyl)<sup>16</sup> (Scheme 2) has allowed a much broader range of monomers like styrene,<sup>17</sup> acrylates,<sup>17</sup> and more recently dimethylacrylamide<sup>18,19</sup> and acrylic acid<sup>20,21</sup> to be controlled.

Most of the NMP studies and main achievements were performed under homogeneous polymerization conditions (i.e., bulk or solution), but recently scientists and industrial partners have directed their research toward NMP in aqueous dispersed media<sup>22,23</sup> like sus-

**Scheme 1. Activation–Deactivation Equilibrium in Nitroxide-Mediated Controlled Free-Radical Polymerization ( $K = k_d/k_c$ )**



**Scheme 2. Structure of the SG1 Nitroxide and of the SG1-Based Water-Soluble Alkoxyamine Initiator (A-H for the Displayed Acidic Form; A-Na for the Corresponding Sodium Salt)**

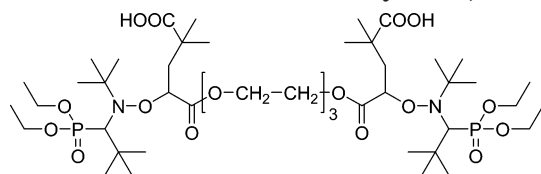


pension, miniemulsion, and emulsion polymerizations.<sup>24–27</sup> Among these “green chemistry”-labeled processes, miniemulsion polymerization was the most studied as it allowed the difficulties and limitations encountered in ab initio emulsion polymerization to be overcome. It indeed represents a simplified model for emulsion polymerization with regards to the nucleation step.<sup>28–30</sup> Even though miniemulsion is an efficient method for encapsulation,<sup>31–36</sup> it is not, for the moment, an industrially viable process since a high shear apparatus is required, and a volatile organic compound as hydrophobic additive is generally used. Consequently, the successful application of NMP in true emulsion polymerization is highly desirable. However, very few articles have reported such an achievement, and none of them was able to produce latexes with simultaneously a high solids content with well-defined (co)polymers (in particular a block copolymer) and a narrow particle size distribution with a controlled average diameter.<sup>37–40</sup>

<sup>†</sup> Université Pierre et Marie Curie.

<sup>‡</sup> ARKEMA.

\* To whom correspondence should be addressed.

**Scheme 3. Structure of the Novel SG1-Based Water-Soluble Difunctional Alkoxyamine, DIAMA**

Recently, our group proposed a simple way to perform nitroxide-mediated emulsion polymerization of both *n*-butyl acrylate and styrene, using a novel water-soluble alkoxyamine based on the nitroxide SG1 (A-Na, the sodium salt of A-H, which is shown in Scheme 2).<sup>41</sup> To avoid droplet nucleation, which appeared to be the main drawback in *ab initio* batch emulsion polymerization mediated by a nitroxide (leading to latex destabilization),<sup>25</sup> a multistep process was applied, starting with the formation of a very dilute seed latex, in which the particles were composed of living oligomeric alkoxyamines. In the second step, the monomer was introduced in one shot, and the final latex resulting from the corresponding seeded emulsion polymerization was stable, with solids content up to 26 wt %. The particle diameters were in the 250–600 nm range with, however, a broad particle size distribution. In all cases, a good control over the molar mass and molar mass distribution was achieved, and an example of diblock copolymer was presented.

In parallel, we have also demonstrated the possibility to achieve surfactant-free batch emulsion polymerization of *n*-butyl acrylate and styrene using a SG1-capped poly(sodium acrylate) macroalkoxyamine as a water-soluble initiator.<sup>42</sup> Despite a rather low initiator efficiency (especially with styrene), stable, 20 wt % solids latexes were recovered with small particles (diameter below 100 nm) and narrow particle size distribution. Because of the high water solubility of the polyelectrolyte macroinitiator, droplet nucleation was not significant, hence allowing stable latexes to be formed in an *ab initio* batch process. The particles were solely stabilized by the charged hydrophilic segments coming from the macroinitiator and covalently attached at the chain end. Nevertheless, a drawback of the high water solubility was the low initiator efficiency due to non-negligible aqueous phase termination reactions.

Consequently, to combine both the macromolecular and colloidal properties derived from these two different systems and to synthesize more complex architectures, the idea was to investigate the effect of a new SG1-based water-soluble difunctional alkoxyamine (called DIAMA, Scheme 3). This dialkoxyamine contains two carboxylic

acid functions separated by an oligo(ethylene glycol)-based diester. The sodium salt form of the DIAMA (called DIAMA-Na) and the derived initiating radical are both water-soluble with two charges in their structure. This might have a highly favorable effect on particle stabilization.

This paper presents the synthesis of the novel difunctional alkoxyamine and its application to the emulsion polymerization of styrene and *n*-butyl acrylate. Syntheses of poly(*n*-butyl acrylate) and polystyrene homopolymers as well a triblock copolymer were investigated, and full attention was given to polymer characterization and colloidal properties of the final latexes in terms of stability, particle size, and particle size distribution.

## Experimental Section

**Materials.** *n*-Butyl acrylate (BA, Aldrich, 99%) and styrene (S, Aldrich, 99%) monomers were distilled under reduced pressure before use. The tri(ethylene glycol) diacrylate (Aldrich) and *tert*-butyl alcohol (Aldrich, 99+%) were used as received. The surfactant Dowfax 8390 (a mixture of mono- and dihexadecyl disulfonated diphenyloxide disodium salt, supplied by Dow Chemical Co.; aqueous solution at 35 wt %; cmc = 0.05 wt % at 25 °C, approximately 0.5–1 mM) and the buffer, sodium hydrogen carbonate (NaHCO<sub>3</sub>, Prolabo, >99%) were used as received. The SG1-based alkoxyamine derived from methacrylic acid, A-H (also called MAMA or BlocBuilder, 99%), was kindly supplied by Arkema (see Scheme 2).

**Syntheses of the SG1-Based Water-Soluble Dialkoxyamine.** A typical procedure for the synthesis of the novel SG1-based difunctional alkoxyamine (DIAMA) is the following. The tri(ethylene glycol) diacrylate (11.01 g, 4.27 × 10<sup>-2</sup> mol) was dissolved in *tert*-butyl alcohol (156.62 g, 2.11 mol), and the mixture was deoxygenated by nitrogen bubbling for 20 min. The alkoxyamine A-H (33.67 g, 8.79 × 10<sup>-2</sup> mol) was then added to the solution in a very slight excess amount with respect to the acrylate functions (1.03 equiv). After complete dissolution, the mixture was poured into a 300 mL glass reactor stirred at 300 rpm, deoxygenated by nitrogen bubbling for 25 min, and then heated at 100 °C. After 1 h, the reaction was stopped by cooling the reaction medium in iced water, and the solution was further concentrated by vacuum evaporation. The product was then purified by three precipitation/filtration cycles in cold pentane and dried at room temperature under vacuum for several days. The purified dialkoxyamine, a white and bright fine powder, was analyzed by <sup>1</sup>H NMR: δ (ppm, 250 MHz, CDCl<sub>3</sub>): 0.5–1.4 (60H, PO(OCH<sub>2</sub>CH<sub>3</sub>)<sub>2</sub>, C(CH<sub>3</sub>)<sub>3</sub>), C(COOH)(CH<sub>3</sub>)<sub>2</sub>), 2.0–2.6 (4H, CH<sub>2</sub>C(COOH)(CH<sub>3</sub>)<sub>2</sub>), 3.1–3.4 (2H, NCHP), 3.5–3.8 (8H, CH<sub>2</sub>OCH<sub>2</sub>CH<sub>2</sub>OCH<sub>2</sub>-), 3.8–4.3 (12H, COOCH<sub>2</sub>CH<sub>2</sub>, PO(CH<sub>2</sub>CH<sub>3</sub>)<sub>2</sub>), 4.3–4.6 (2H, NOCHCOO), 8.4–9.4 (2H, COOH).

**Bulk Polymerization.** In a typical experiment (experiment 1<sub>BA</sub>, Table 1), a mixture of the DIAMA alkoxyamine (2.45 g, 2.47 × 10<sup>-3</sup> mol) and *n*-butyl acrylate (82.0 g, 0.64 mol) was deoxygenated by nitrogen bubbling for 20 min at room tem-

**Table 1. Experimental Conditions for the SG1-Mediated Bulk, Batch Emulsion, and Seeded Emulsion Polymerizations at 112 °C**

expt	process	alkoxyamine initiator type (mol L <sup>-1</sup> <sub>aq</sub> )	seed latex	monomer(s)	monomer content (wt %)	target DP <sub>n</sub> at 100% conv	[surfactant] mol L <sup>-1</sup> <sub>aq</sub> (wt %) <sup>a</sup>	time (h)
1 <sub>BA</sub>	bulk	DIAMA		BA	100	259		3
1 <sub>S</sub> <sup>b</sup>	bulk	DIAMA		S	100	320		2
2	batch emulsion	DIAMA-Na (5.7 × 10 <sup>-3</sup> )		BA	0.7	10	6.9 × 10 <sup>-3</sup>	8
3	batch emulsion	DIAMA-Na (5.7 × 10 <sup>-3</sup> )		BA	0.7	10	3.0 × 10 <sup>-3</sup>	8
4	batch emulsion	DIAMA-Na (5.6 × 10 <sup>-3</sup> )		BA	0.7	10	1.5 × 10 <sup>-3</sup>	8
5	seeded emulsion	DIAMA-Na (5.7 × 10 <sup>-3</sup> )	2	BA + BA	16	268	6.9 × 10 <sup>-3</sup> (2.3)	8
6	seeded emulsion	DIAMA-Na (5.7 × 10 <sup>-3</sup> )	3	BA + BA	16	268	6.9 × 10 <sup>-3</sup> (2.3)	8
7	seeded emulsion	DIAMA-Na (5.6 × 10 <sup>-3</sup> )	4	BA + BA	16	269	6.8 × 10 <sup>-3</sup> (2.3)	8
8	seeded emulsion	DIAMA-Na (5.6 × 10 <sup>-3</sup> )	4	BA + S	16	332	1.5 × 10 <sup>-2</sup> (5.0)	8
9	seeded emulsion	DIAMA-Na (5.5 × 10 <sup>-3</sup> )	4	BA + S	16	338	6.7 × 10 <sup>-3</sup> (2.2)	8
10	seeded emulsion	DIAMA-Na (5.6 × 10 <sup>-3</sup> )	4	BA + BA + S	26	506	1.2 × 10 <sup>-2</sup> (2.3)	14

<sup>a</sup> Based on the overall weight of monomer. <sup>b</sup> 120 °C.

perature. The medium was poured into a 300 mL thermostated glass reactor heated at 112 °C and then stirred at 300 rpm. Time zero of the reaction corresponded to the introduction of the mixture in the preheated reactor. Samples were periodically withdrawn to monitor the monomer conversion by gravimetry. For this purpose, the samples were dried in a ventilated oven thermostated at 70 °C, until constant weight. After drying, the raw polymer from each sample was analyzed by size exclusion chromatography for molar mass and molar mass distribution measurement. The same experimental protocol was applied for the bulk polymerization of styrene at 120 °C (experiment 1<sub>S</sub> see Table 1).

**Emulsion Polymerization.** The seed latexes were prepared in a 600 mL thermostated glass PARR reactor; the seeded emulsion polymerizations were performed in the same reactor, using a 300 mL glass tank.

**Seed Latex.** In a typical experiment (experiment 2, Table 1), an aqueous emulsion of the monomer was prepared by mixing BA (3.0 g,  $5.6 \times 10^{-2}$  mol L<sup>-1</sup>, 0.70 wt %) with the water phase (400 mL) containing the Dowfax 8390 surfactant (1.87 g,  $6.88 \times 10^{-3}$  mol L<sup>-1</sup>) and NaHCO<sub>3</sub> ( $1.2 \times 10^{-2}$  mol L<sup>-1</sup>). The mixture was deoxygenated by nitrogen bubbling for 20 min and then poured into the reactor, preheated at 112 °C, and stirred at 300 rpm. The acidic DIAMA alkoxyamine (2.35 g,  $2.37 \times 10^{-3}$  mol), neutralized with an excess (1.60 equiv with respect to the acidic functions) of a 0.4 M sodium hydroxide solution (giving the corresponding DIAMA-Na), was introduced into the reactor when the temperature reached 90 °C, triggering the beginning of the reaction. Afterward, a 3 bar pressure of nitrogen was applied. After 8 h of polymerization, the reactor was cooled in an iced water bath. The latex was analyzed by dynamic light scattering to determine the average particle size. The dried polymer was further analyzed by SEC (size exclusion chromatography), and final conversion was determined by gravimetry.

**Seeded Emulsion Polymerization:** In a typical experiment (experiment 5, Table 1) a fraction (160 g) of the seed latex **2** prepared in a first step was poured into the reactor, already heated at 112 °C. When temperature of the mixture reached 90 °C, representing the time zero of the reaction, a "one-shot" addition of *n*-butyl acrylate (29.2 g, 0.23 mol) was performed (representing 16 wt % solids in the final latex), and a 3 bar pressure of nitrogen was applied. Samples were periodically withdrawn to monitor the monomer conversion by gravimetry. The dried polymer was further analyzed by SEC. The latexes were analyzed by dynamic light scattering to determine the average particle size. For the other seeded emulsion polymerizations performed from the seed latexes **3** and **4** (i.e., experiments 6–9), as a variable part of the surfactant was introduced in the first step (synthesis of the seed), the remaining part was added just before the second step (seeded emulsion polymerization), so as to reach an overall amount of 2.3 wt % based on the monomer (experiments 6, 7, and 9) or of 5.0 wt % (experiment 8).

**Synthesis of a Triblock Copolymer in Emulsion Polymerization.** The multistep emulsion polymerization process was applied to the synthesis of a triblock copolymer with a 1:1 molar ratio of styrene and *n*-butyl acrylate (experiment 10, Table 1). (i) Synthesis of the poly(*n*-butyl acrylate) central block: A part (130 g) of the seed latex **4** was poured into the reactor, already heated at 112 °C. A load of surfactant was added (0.43 g,  $6.7 \times 10^{-4}$  mol) so as to reach 2.2 wt % of Dowfax 8390 with respect to the overall *n*-butyl acrylate. When the temperature of the mixture reached 90 °C, representing the time zero of the reaction, a "one-shot" addition of *n*-butyl acrylate (24.5 g, 0.19 mol) was performed (representing 16 wt % solids in the final latex), and a 3 bar pressure of nitrogen was applied. Before the end of this second step (6 h, 71% BA conversion), the polymerization was stopped by cooling the reaction medium. (ii) Synthesis of the external polystyrene blocks: The unreacted BA was not removed, and another load of surfactant was added (0.43 g,  $6.7 \times 10^{-4}$  mol) so as to reach again a concentration of 2.2 wt % of Dowfax 8390 with respect to the overall monomers BA and S. Part of the styrene (1.9 g,  $1.83 \times 10^{-2}$  mol, 10 wt % based on the overall required styrene)

was added into the cooled latex and gentle stirring was applied overnight at room temperature. After addition of the remaining styrene (17.2 g, 0.17 mol), the temperature was raised again to 112 °C to resume the polymerization. The target overall composition of the copolymer was 1:1, mol:mol (55 wt % of BA). Samples were periodically withdrawn throughout the two steps to monitor the monomer conversion by gravimetry. The dried polymer was further analyzed by SEC, and the latexes were analyzed by dynamic light scattering to determine the average particle size.

**Analytical Techniques.** The particle diameter was measured by dynamic light scattering (DLS) with a Zetasizer4 from Malvern ( $\lambda = 670$  nm, 3 mW, 90° scattering angle) at a temperature of 25 °C. Before measurements, the latex samples were diluted in deionized water. For polystyrene latexes only, transmission electron microscopy was used (TEM, JEOL 100 Cx II at 100 keV with a high-resolution CCD camera KeenView from SIS) with a counting over more than 500 particles (not all shown in Figure 8). Calibration was previously performed using three well-defined polystyrene particle samples supplied by Ted Pella Inc. (PELCO 610-SET: 91, 300, and 482 nm).

Size exclusion chromatography was performed at 40 °C with two columns (PSS SDV, linear MU, 8 mm  $\times$  300 mm; bead diameter: 5  $\mu$ m; separation limits: 400– $2 \times 10^6$  g mol<sup>-1</sup>). The eluent was tetrahydrofuran (THF) at a flow rate of 1 mL min<sup>-1</sup>. A differential refractive index detector (LDC Analytical refractoMonitor IV) was used, and molar mass distributions were derived from a calibration curve based on polystyrene standards from Polymer Standards Service. This technique allowed  $M_n$  (the number-average molar mass),  $M_w$  (the weight-average molar mass), and PDI =  $M_w/M_n$ , the polydispersity index to be determined.<sup>43</sup>

<sup>1</sup>H NMR spectroscopy (250 MHz) analyses were performed in CDCl<sub>3</sub> solution, at 25 °C, in 5 mm tubes, using an AC250 Bruker spectrometer.

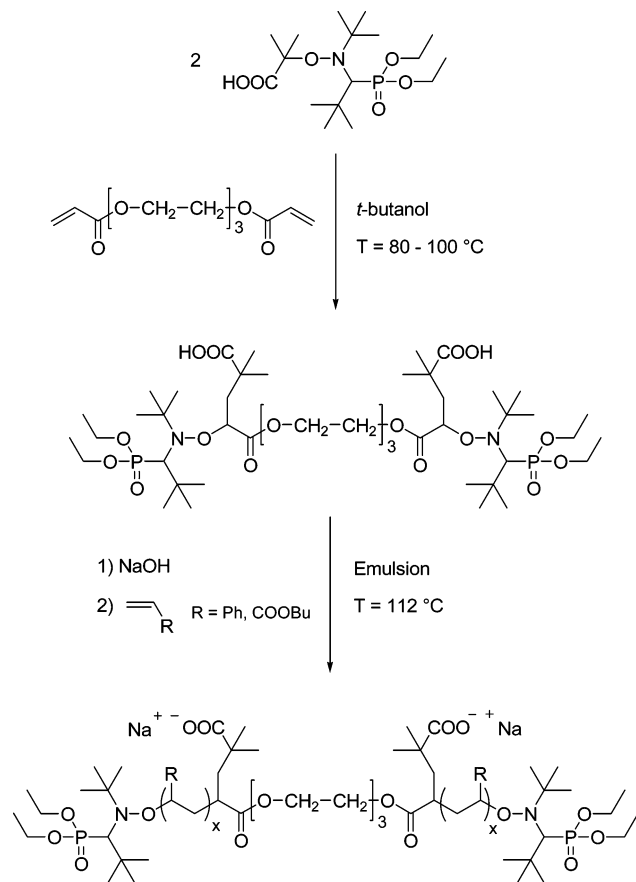
The liquid adsorption chromatography (LAC) analysis was performed in the Groupement de Recherches de Lacq (Arke-ma). Separation was carried out with a grafted silica column using a gradient hexane/THF solvent mixture as an eluent at 30 °C and at a flow rate of 3 mL min<sup>-1</sup>. The detection was performed using a UV detector (Waters 481 Spherisorb S5 CN) and an evaporative light scattering detector (DEDL 21, Eurosep). Details on the experimental conditions can be found in ref 44.

## Results and Discussion

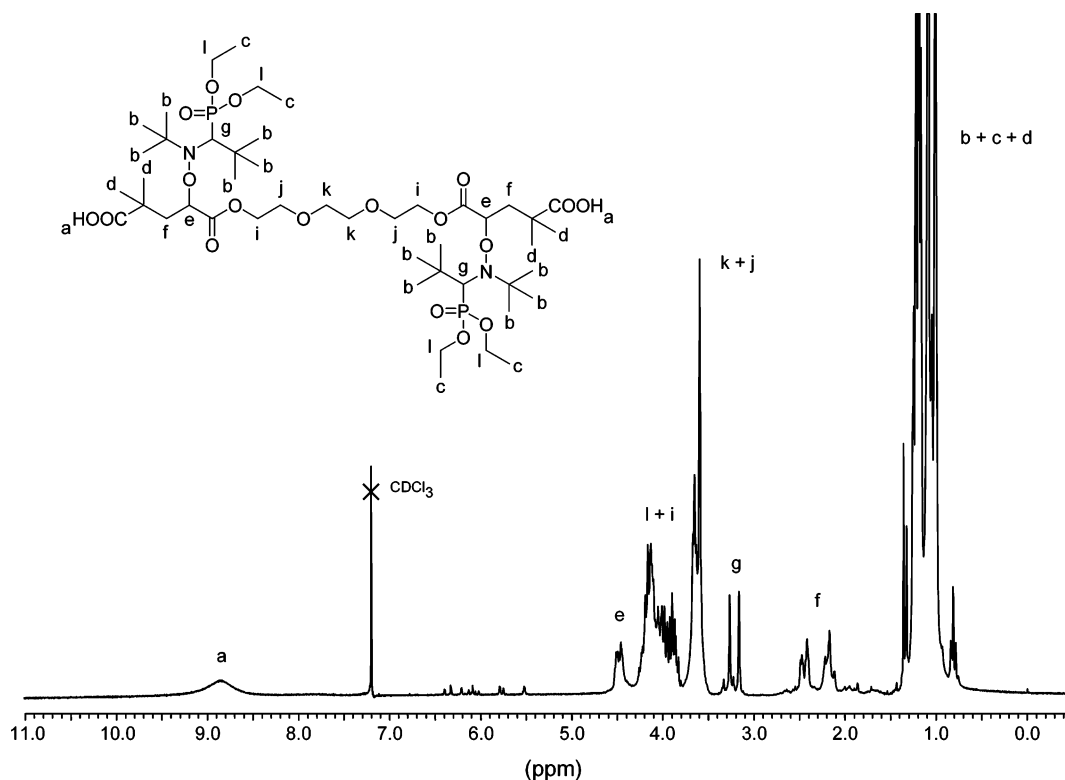
### 1. Synthesis and Characterization of the Novel SG1-Based Water-Soluble Dialkoxyamine DIAMA.

An overview of the dialkoxyamine synthesis is presented in Scheme 4. The concept of the synthesis is the following. Because of the low cleavage temperature of the starting A-H alkoxyamine ( $T_c < 50$  °C, estimated by monitoring with ESR the signal of the released nitroxide moiety),<sup>45</sup> intermolecular radical 1,2-addition can be performed on an activated olefin in order to produce a new alkoxyamine with a lower dissociation rate constant, which would be stable at the reaction temperature.<sup>46</sup> Because of the high dissociation rate constant of the A-H alkoxyamine,<sup>45</sup> a high concentration of SG1 is released at the onset of the reaction. The persistent radical effect<sup>47</sup> is then strongly pronounced, and neither oligomerization nor dimerization is expected. We decided to adapt this chemistry for the synthesis of a novel SG1-based water-soluble alkoxyamine, intended to be used as an initiator in emulsion polymerization. To produce complex architectures like triblock copolymers, the activated olefin moiety was purposely chosen to be difunctional. Two molar equivalents of the A-H alkoxyamine was reacted with tri-(ethylene glycol) diacrylate at 100 °C for 1 h so as to perform a double intermolecular radical 1,2-addition.



**Scheme 4. Synthesis and Use as an Initiator of the Novel SG1-Based Water-Soluble Difunctional Alkoxyamine, DIAMA**

The purified product was obtained with correct yield ( $\sim 70\%$ ), and its  $^1\text{H}$  NMR characterization agreed well with the expected dialkoxyamine structure (Figure 1).

**Figure 1.** 250 MHz  $^1\text{H}$  NMR spectrum of the purified SG1-based dialkoxyamine, DIAMA.

No remaining A-H alkoxyamine could be detected.<sup>48</sup> Residual peaks corresponding to unreacted vinylic functions were also observed ( $\delta$  5.5–6.5 ppm). On the basis of the reasonable hypothesis that one diacrylate molecule has reacted at least once with the A-H alkoxyamine, one can determine the relative proportions of target dialkoxyamine (derived from a double radical addition) and of monoalkoxyamine (derived from a single radical addition). By integrating the  $^1\text{H}$  NMR signal corresponding to the vinylic protons and to a characteristic proton from SG1 (peaks *g*, Figure 1), the molar fraction of DIAMA was estimated at 92 mol %. Titration of the dialkoxyamine in absolute ethanol by 0.1 M sodium hydroxide solution also confirmed the expected concentration of acidic protons, with  $\text{p}K_{\text{a}} = 5.55$ .<sup>49</sup> This value is consistent with the lower  $\text{p}K_{\text{a}} = 4.98$  found for the A-H alkoxyamine, following the same titration procedure,<sup>41</sup> owing to a higher electronic density on the acidic protons of the DIAMA.

Because of the simple synthesis procedure, the method is quite versatile and could be applied to the preparation of a variety of mono- or multifunctional alkoxyamines.<sup>46</sup>

**2. Bulk Polymerizations of *n*-Butyl Acrylate and Styrene.** In a preliminary study, the DIAMA was first used as a difunctional initiator in the bulk polymerization of *n*-butyl acrylate at 112  $^{\circ}\text{C}$  and styrene at 120  $^{\circ}\text{C}$  (experiments 1<sub>BA</sub> and 1<sub>S</sub>, respectively; see Table 1 and Figure 2). The polymerizations were fast, with 80% monomer conversion within 3 h for BA and 2 h for S. The logarithmic conversion exhibited a linear evolution with time (slope:  $k_{\text{p}}[\text{P}^{\bullet}] = 1.45 \times 10^{-4} \text{ s}^{-1}$  with a correlation coefficient  $R^2 = 0.997$  for BA and  $2.12 \times 10^{-4} \text{ s}^{-1}$  with  $R^2 = 0.990$  for S). One can then calculate the proportion of free SG1 (already present as an impurity in the DIAMA or most probably released during the polymerization owing to the irreversible macroradical self-terminations—the so-called persistent radical effect<sup>47</sup>) with respect to the initial alkoxyamine functions

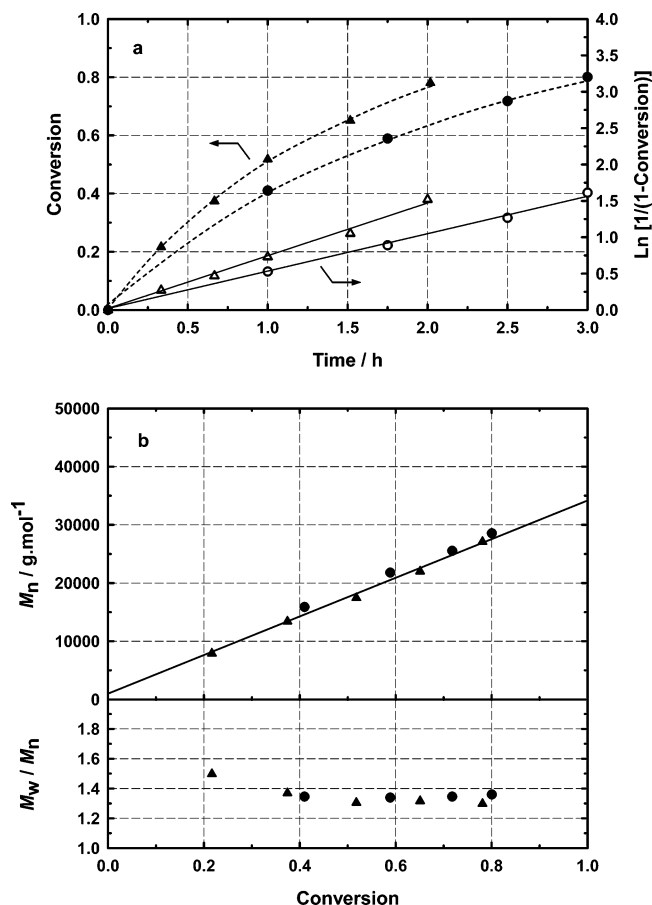


**Figure 2.** Bulk polymerization of *n*-butyl acrylate (experiment 1<sub>BA</sub>: ●, ○) and styrene (experiment 1<sub>S</sub>: ▲, △) initiated by the difunctional SG1-based alkoxyamine DIAMA: (a) monomer conversion and logarithmic conversion vs time; (b) number-average molar mass,  $M_n$ , and polydispersity index,  $M_w/M_n$ , vs conversion. Full straight line: theoretical evolution of  $M_n$  vs conversion.

for both experiments. (i) For *n*-butyl acrylate:  $[\text{SG1}]/(2 \times [\text{DIAMA}]_0) = (K \times f)/[\text{P}^*] = 0.023$ , with the activation–deactivation equilibrium constant<sup>50</sup>  $K = 4.34 \times 10^{-11} \text{ mol L}^{-1}$  and the propagation rate constant<sup>51</sup>  $k_p = 82\,000 \text{ L mol}^{-1} \text{ s}^{-1}$  at 112 °C; the initiator efficiency,  $f = 0.95$ , was determined from the ratio of the theoretical molar masses over the experimental ones. The low proportion of released SG1 indicates that the polymerization of *n*-butyl acrylate proceeded almost ideally, in the absence of extensive termination reactions. The latter could even be reduced, but at the expense of the polymerization rate, if free SG1 was initially added in the polymerization medium.<sup>52</sup> (ii) For styrene:  $[\text{SG1}]/(2 \times [\text{DIAMA}]_0) = (K \times f)/[\text{P}^*] = 0.058$ , with the activation–deactivation equilibrium constant<sup>17</sup>  $K = 6.0 \times 10^{-9} \text{ mol L}^{-1}$  and the propagation rate constant<sup>53</sup>  $k_p = 2036 \text{ L mol}^{-1} \text{ s}^{-1}$  at 120 °C; the efficiency  $f = 1$ . The trend for styrene polymerization to exhibit a larger proportion of free SG1 (i.e., a larger proportion of dead chains) is not unexpected and is directly correlated with the higher  $K$  value.

The evolution of the molar masses was linear with monomer conversion and followed quite closely the predicted values; i.e., the initiator efficiency was very high ( $f = 0.95$  for BA and  $f = 1$  for S). The polydispersity indexes remained quite low for this kind of architecture even for large conversion (PDI was between 1.3 and 1.4 at 80% conversion), but they were generally above those

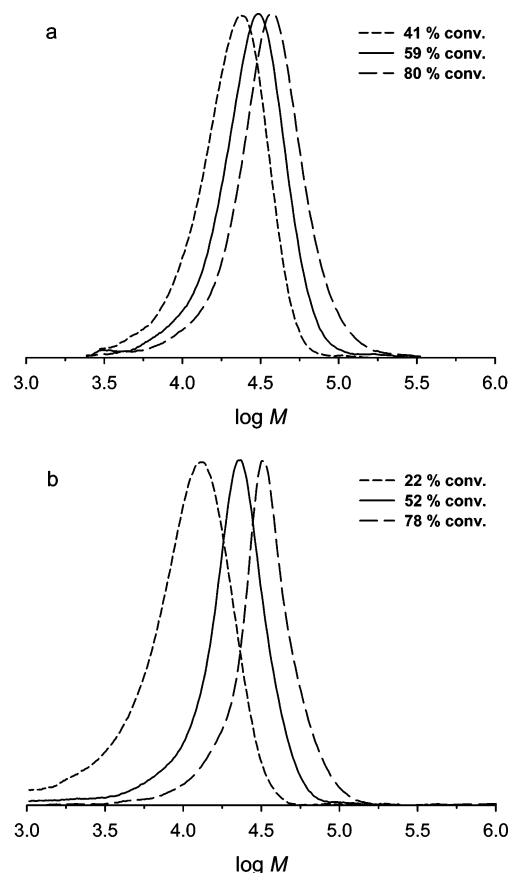


**Figure 3.** Size exclusion chromatograms recorded at various conversions for the bulk polymerizations of *n*-butyl acrylate (a, experiment 1<sub>BA</sub>) and styrene (b, experiment 1<sub>S</sub>) initiated by the DIAMA.

found with the monofunctional A-H alkoxyamine (generally below 1.2), under otherwise unchanged experimental parameters.<sup>54</sup> This is first explained by the fact that the dialkoxyamine contains a proportion of mono-alkoxyamine (leading to chains growing on a single side, with half the expected length) and second by the possibility for the growing chains to undergo recombination reactions more than once, still keeping their difunctional character, whereas only one recombination is allowed for a monofunctional growing chain. However, the continuous shift of the size exclusion chromatograms demonstrates the “living” character of the polymerizations (Figure 3).

### 3. Homopolymerization of *n*-Butyl Acrylate and Styrene in a Two-Step Emulsion Polymerization Process. Synthesis of the Seed Latex.

Like the A-Na alkoxyamine initiator, the DIAMA-Na was not able to produce stable latexes via a simple *ab initio* batch emulsion polymerization process. Consequently, emulsion polymerizations were performed using a two-step process starting with a very dilute monomer-in-water emulsion polymerization (to form the so-called “living” seed latex), followed by monomer addition to reach higher solids content as well as higher molar masses. This process has been previously applied to form a “living” poly(*n*-butyl acrylate) seed latex initiated by the A-Na alkoxyamine (Scheme 2).<sup>41</sup> After a “one-shot” monomer addition (either *n*-butyl acrylate or styrene), stable latexes were obtained, and it was shown that the final average diameter was strongly dependent on the initial surfactant concentration used in the seed. Unfortunately, rather broad particle size distribution was

**Table 2. Final Conversion and Colloidal Characteristics of the SG1-Mediated Seeded Emulsion Polymerization Latexes**

expt	conv (%)	final $N_p$ from DLS <sup>a</sup> ( $10^{16} \text{ L}^{-1} \text{ emulsion}$ )	final DLS data		final TEM data <sup>c</sup>		
			$D_z$ (nm)	polydispersity ( $\sigma$ ) <sup>b</sup>	$D_n$ (nm)	$D_w$ (nm)	polydispersity index ( $\gamma$ )
2	58	3.2	60	0.202			
3	52	1.3	80	0.222			
4	54	0.17	155	0.114			
5	89	5.0	170	0.062			
6	89	3.3	195	0.052			
7	88	1.3	265	0.097			
8	87	1.0	290	0.130	250	370	1.48
9	86	1.3	270	0.048	280	330	1.18
10	85	1.4	300	0.115			

<sup>a</sup>  $N_p$  was calculated using  $N_p = (6\tau_p)/(\pi d_p D_z^3)$  with  $\tau_p$  the polymer content,  $d_p$  the polymer density, and  $D_z$  the average diameter given by DLS. <sup>b</sup>  $\sigma$ , given by the DLS apparatus, characterizes the particle size distribution ( $0 < \sigma < 1$ ); it corresponds to the ratio of the variance over the square of the average particle diameter. The particle size distribution is generally considered as monodisperse and narrow when  $\sigma$  is below 0.10. <sup>c</sup>  $D_n = \sum_i n_i D_i / \sum_i n_i$ ,  $D_w = \sum_i n_i D_i^4 / \sum_i n_i D_i^3$ ; polydispersity index  $\gamma = D_w/D_n$ .

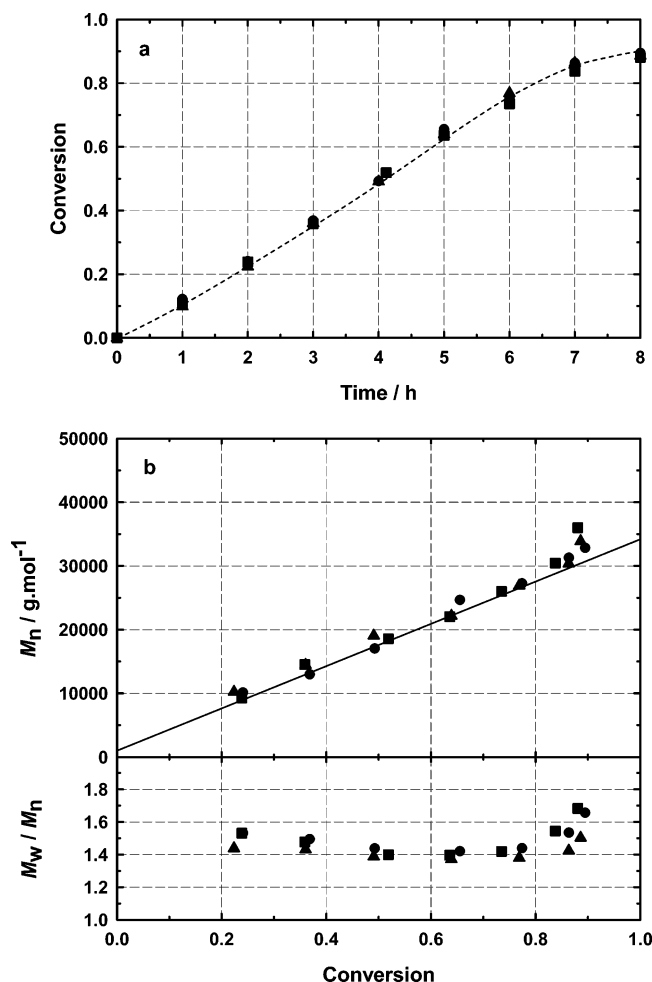


**Figure 4.** Seeded emulsion polymerizations of *n*-butyl acrylate (experiment 5,  $\blacktriangle$ ; experiment 6,  $\bullet$ ; experiment 7,  $\blacksquare$ ) initiated by the difunctional SG1-based water-soluble alkoxyamine DIAMA-Na: (a) monomer conversion vs time; (b) number-average molar mass,  $M_n$ , and polydispersity index,  $M_w/M_n$ , vs conversion. Full straight line: theoretical evolution of  $M_n$  vs conversion.

observed in all cases. To establish comparisons with the A-Na alkoxyamine, we decided to investigate the use of the DIAMA-Na as a difunctional SG1-based water-soluble alkoxyamine in emulsion polymerization, following exactly the same procedure (see the Experimental Section). Three poly(*n*-butyl acrylate) seeds, differing only by the concentration of surfactant, were synthesized (experiments 2–4, Table 1). After 8 h of polymerization, the latexes were stable with a final conversion in BA around 55%. As expected, the synthesized

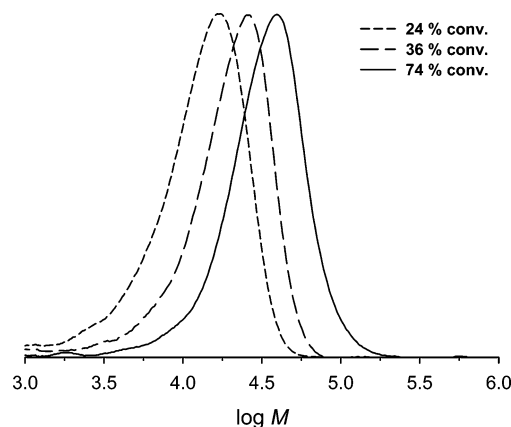


**Figure 5.** Size exclusion chromatograms recorded at various conversions for the seeded emulsion polymerization of *n*-butyl acrylate initiated by DIAMA-Na (experiment 7).

oligomers exhibited molar masses close to the theoretical ones (for experiment 2, theoretical  $M_n = 1720 \text{ g mol}^{-1}$  at 55% conversion; the experimental molar mass at the maximum of the SEC peak was  $M_p = 1730 \text{ g mol}^{-1}$ , whereas  $M_n$  was about  $1400 \text{ g mol}^{-1}$ , with however a low accuracy owing to the difficulty in selecting precisely the lower mass limit of the peak). From DLS (Table 2), it was shown that the final average diameter increased (from 60 nm for experiment 2 to 155 nm for experiment 4) when the surfactant concentration was decreased. When compared to A-Na alkoxyamine under otherwise unchanged experimental conditions (experiment 1 in ref 41), the very interesting result is that the DIAMA-Na has permitted the average particle diameter in the seed latex to be drastically decreased (210 nm with the A-Na vs 60 nm with the DIAMA-Na in experiment 2, under the same surfactant concentration). It has been previously mentioned that the negative charge coming from the A-Na initiator attached at the chain end contributed to enhance the particle stabilization as proven by capillary hydrodynamic fractionation analyses and surface tension measurements.<sup>54</sup> Thus, it can be inferred that the double negative charge of the DIAMA-Na, which is covalently bound to the polymer chain upon initiation and propagation, may have an even better influence, as it forces a larger proportion of charges to remain locked at the particle surface and to contribute to the stabilization by electrostatic repulsion. However, particle size is still too large for all chain ends to be located at the particle surface, and part of the oligomers should remain buried inside the latex particle.

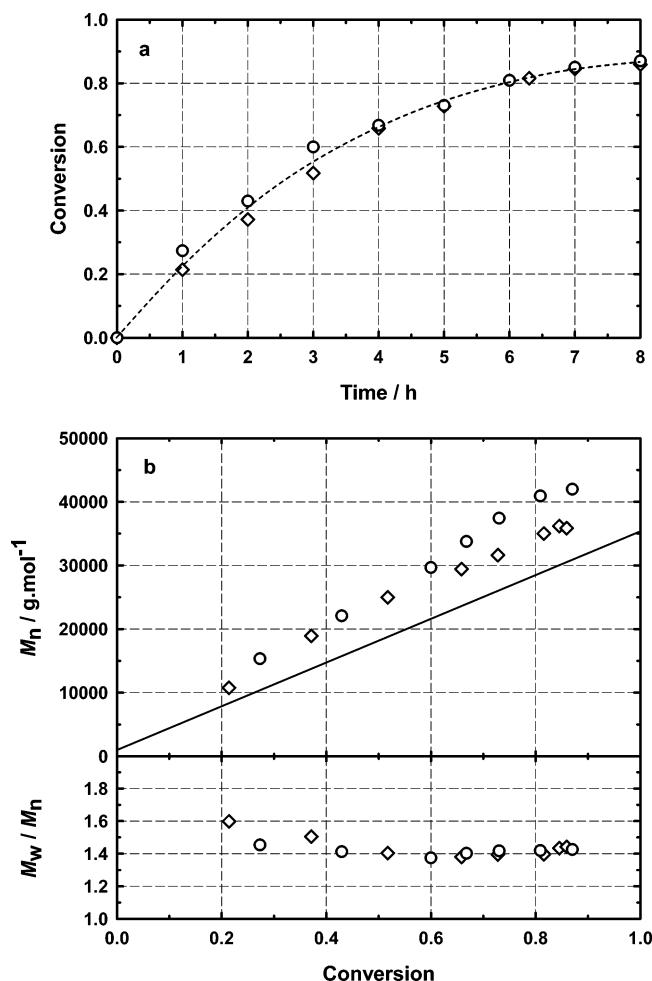


**Figure 6.** Seeded emulsion polymerizations of styrene (experiment 8,  $\circ$ ; experiment 9,  $\diamond$ ) initiated by the difunctional SG1-based water-soluble alkoxyamine DIAMA-Na: (a) monomer conversion vs time; (b) number-average molar mass,  $M_n$ , and polydispersity index,  $M_w/M_n$ , vs conversion. Full straight line: theoretical evolution of  $M_n$  vs conversion.

**Seeded Emulsion Polymerizations of *n*-Butyl Acrylate.** The low solids content poly(*n*-butyl acrylate) seed latexes produced in the previous step were further extended by a “one shot” BA addition through a batch seeded emulsion polymerization to target 16 wt % solids content (experiments 5–7, Table 1). Before monomer addition, a new load of surfactant was added for experiments 6 and 7 (extended respectively from the seed latexes 3 and 4) so as to reach the same aqueous concentration as in experiment 5 (from the seed latex 2 with the highest surfactant initial concentration), i.e.,  $6.9 \times 10^{-3} \text{ mol L}^{-1}$ . After polymerizations, stable latexes were recovered with neither coagulum nor destabilization over time. As illustrated in the conversion vs time plots (Figure 4), reactions were fast (at least for nitroxide-mediated polymerizations) and reached high monomer conversions ( $\sim 90\%$ ). No significant influence of the initial surfactant concentration over the kinetics was detected, i.e., no significant influence of the seed particle size. This result confirms the absence of compartmentalization effect in nitroxide-mediated polymerization performed in aqueous dispersed systems, as the particle number did not influence the polymerization rate.<sup>55</sup> In other words, the kinetics were simply governed by the activation–deactivation equilibrium. Polymers with controlled molar masses and rather low polydispersity indexes were obtained as displayed in Figure 4. The  $M_n$

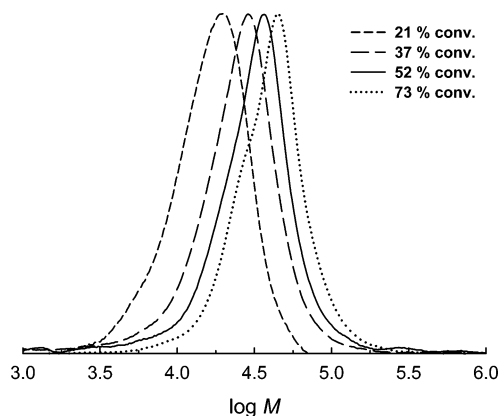


**Figure 7.** Size exclusion chromatograms recorded at various conversions for the seeded emulsion polymerization of styrene initiated by DIAMA-Na (experiment 9).

values increased linearly with monomer conversion and followed the theoretical ones, thus indicating a high initiator efficiency ( $f \sim 1$ ). After 80% conversion, a broadening of the molar mass distribution was significant and possibly due to irreversible termination and/or branching reactions, not unexpected with acrylate monomer at such a high conversion.<sup>56</sup> However, the continuous and complete shift of the size exclusion chromatograms of experiment 7 (Figure 5) also confirmed the “living” character of the polymerization as well as the good reinitiation step from the seed.

From the colloidal viewpoint, the latexes were stable, and it is shown in Table 2 that they exhibited a narrow particle size distribution since  $\sigma$  (polydispersity index taken from the DLS data) was below 0.10 for each of them. Although the concentration of surfactant was the same for all latexes in this second polymerization step, the number of particles  $N_p$  followed the same trend as the seed, from which they originated; i.e.,  $N_p$  was higher when the surfactant concentration in the seed was larger. A more thorough discussion on particle size and number will be presented in point 5 of this section.

**Seeded Emulsion Polymerizations of Styrene.** To demonstrate the flexibility of our process, two types of experiments were then performed with styrene, starting from the poly(*n*-butyl acrylate) seed latex 4 and varying the amount of added surfactant before the second step. Indeed, final surfactant concentrations of 5.0 and 2.2 wt % with respect to the overall monomer were targeted (respectively experiments 8 and 9). No significant influence of the surfactant concentration in the second step was again observed on the monomer conversion vs time plots (Figure 6). In the context of nitroxide-mediated polymerizations, the reactions were fast, and monomer conversion reached  $\sim 90\%$  within 8 h. Control over molar masses and molar mass distribution was good since  $M_n$  increased with monomer conversion, and final PDIs at 85% conversion were as low as 1.44. However, the initiation efficiency was below 1 ( $f = 0.71$  and  $0.87$ , for experiments 8 and 9, respectively) as was also previously observed for the miniemulsion polymerizations of styrene with the A-Na alkoxyamine initiator, indicating potential irreversible terminations of oligoradicals in the aqueous phase.<sup>54</sup> In Figure 7, the continuous evolution of the size exclusion chromatography traces (experiment 9) illustrates the controlled character of the polymerization. However, a slight tailing on the lower molar mass side of the peak is noticed at 73% conversion. As also reported earlier<sup>54</sup> for the miniemulsion polymeriza-



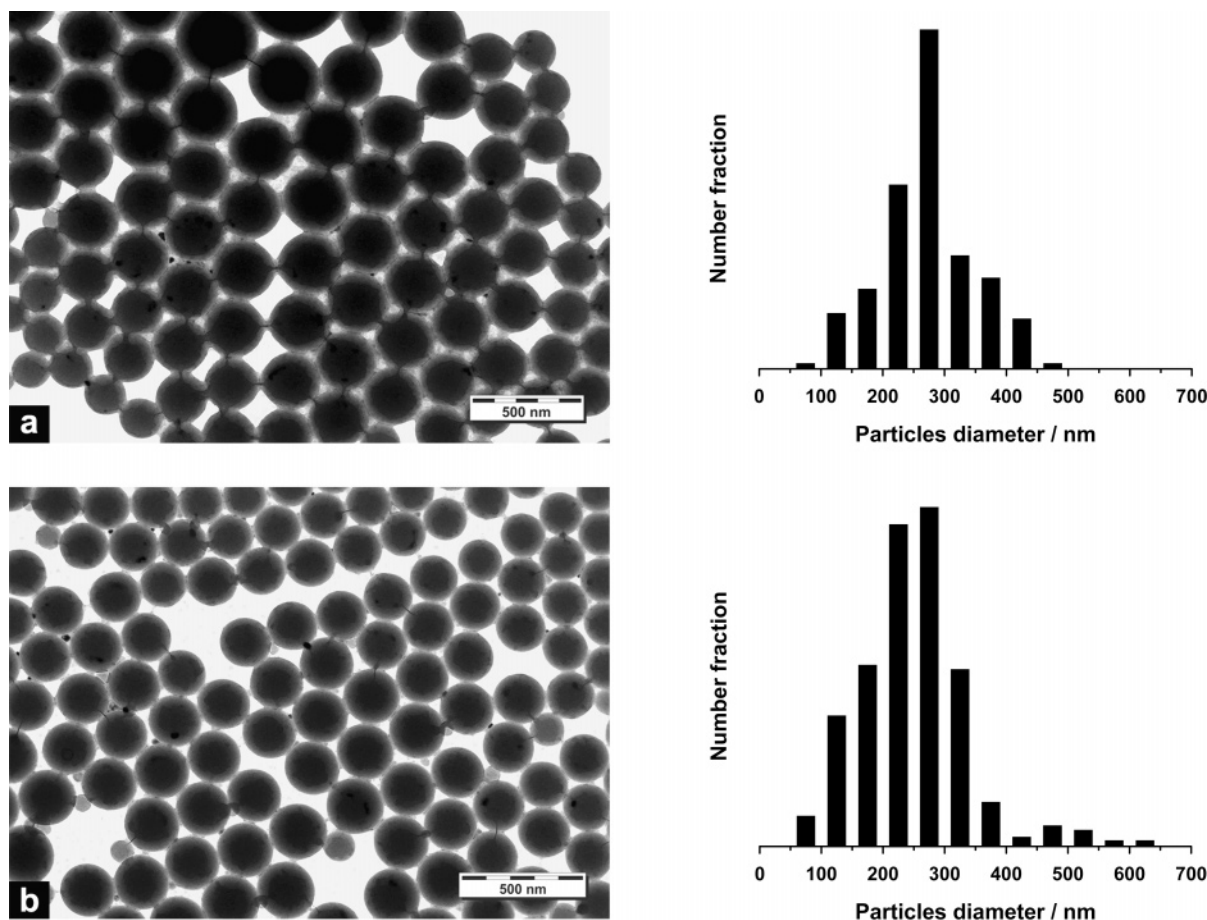


**Figure 8.** Transmission electronic microscopy (TEM) images and associated particle size distributions of the polystyrene particles from experiment 9 (a) and experiment 8 (b).

tions initiated by the A-Na alkoxyamine, the latex pH for styrene remained above 8, whereas with *n*-butyl acrylate it continuously decreased to 6. Thus, with such a high pH in the case of styrene, we might suspect the partial hydrolysis of one ester function of the di-alkoxyamine, hence producing shorter, monofunctional growing chains, detectable on the SEC traces at high conversions.

Transmission electron microscopy (TEM) analysis is possible for the hard polystyrene spheres, and the pictures of the above-presented experiments are displayed in Figure 8. The particle size distribution in experiment 9 was rather homogeneous (Figure 8a) since the polydispersity index,  $\gamma$ , was very close to 1 (1.18) (see Table 2). This was additionally confirmed by the small  $\sigma$  value given by DLS (0.048). The latex from experiment 8 exhibited a rather narrow particle size distribution, too (although broader than experiment 9, owing to the presence of a small fraction of large particles), as we can see on the TEM histogram (Figure 8b) and from the particle size distribution and polydispersity indexes given by the TEM and DLS analyses (Table 2).

**4. Synthesis of a Triblock Copolymer in a Three-Step Emulsion Polymerization Process.** The multistep emulsion polymerization process was then applied to the synthesis of a triblock copolymer based on *n*-butyl acrylate and styrene with a 1:1 molar ratio (experiment 10). Starting from a poly(*n*-butyl acrylate) seed latex (experiment 4), the second step was identical to experiment 7, except it was stopped at 71% BA conversion (6

h) in order to minimize the possible irreversible termination or transfer reactions (Figure 9). Another surfactant addition was performed to reach 2.2 wt % with respect to the overall amount of monomer (BA + S) just before adding styrene and resuming the polymerization. After an additional 8 h, the final global conversion was 85% and a stable latex was recovered with no coagulum. Molar masses increased linearly with monomer conversion following the theoretical values. The polydispersity indexes were below 1.50 until 70% monomer conversion and finally reached 1.64 at 85%. Figure 10 points out the controlled character of the polymerization with the continuous evolution of the size exclusion chromatograms with the global monomer conversion. However, a shoulder on the higher molar mass side of the peak is detectable at 78% conversion certainly due to combination reactions producing pentablocks and thus increasing the molar masses, as well as the polydispersity indexes.

The triblock copolymer was analyzed by liquid adsorption chromatography (LAC), which performs separation according to the chemical composition only. From the chromatograms (Figure 11), no detectable amount of poly(*n*-butyl acrylate) homopolymer was shown, signifying a highly efficient reinitiation by the first block. Furthermore, the copolymer peak was rather narrow and symmetrical, thus indicating a narrow composition distribution.

From  $^1\text{H}$  NMR spectroscopy, the overall copolymer composition was determined, and as expected from the initial amount of monomer, we obtained 49.9 mol % of



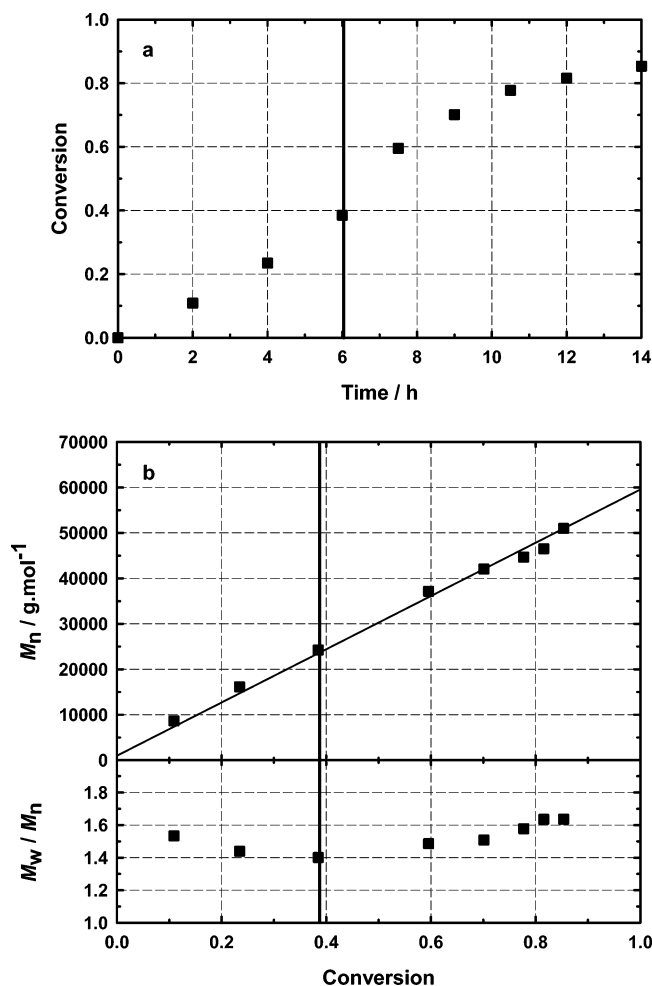


**Figure 9.** Synthesis of a poly(styrene-*co*-*n*-butyl acrylate)-*b*-poly(*n*-butyl acrylate)-*b*-poly(styrene-*co*-*n*-butyl acrylate) block copolymer (experiment 10: ■) in a three-step emulsion polymerization initiated by the difunctional SG1-based water-soluble alkoxyamine DIAMA-Na: (a) monomer conversion vs time; (b) number-average molar mass,  $M_n$ , and polydispersity index,  $M_w/M_n$ , vs conversion. Vertical line: time when styrene was added. Straight line: theoretical evolution of  $M_n$  vs conversion.

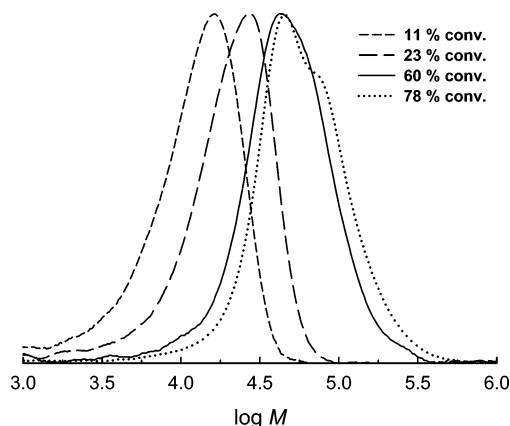


**Figure 10.** Size exclusion chromatograms recorded at various conversions for the synthesis of a poly(styrene-*co*-*n*-butyl acrylate)-*b*-poly(*n*-butyl acrylate)-*b*-poly(styrene-*co*-*n*-butyl acrylate) block copolymer in a seeded emulsion polymerization initiated by DIAMA-Na (experiment 10).

styrene and 50.1 mol % of BA, which leads to the following monomer subunits distribution: P(S<sub>108-co</sub>-BA<sub>17</sub>)-*b*-PBA<sub>182</sub>-*b*-P(S<sub>108-co</sub>-BA<sub>17</sub>).

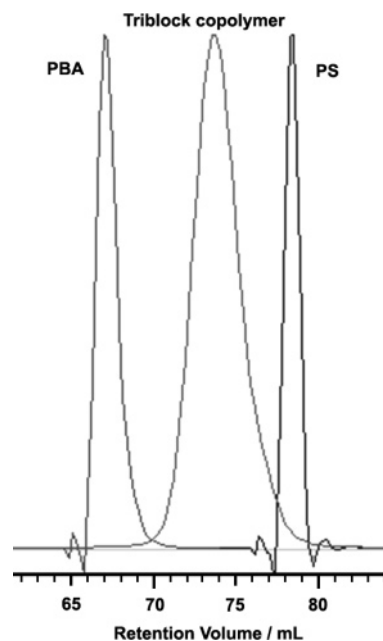


**Figure 11.** Liquid adsorption chromatography traces of the PBA and PS standards and of the poly(styrene-*co*-*n*-butyl acrylate)-*b*-poly(*n*-butyl acrylate)-*b*-poly(styrene-*co*-*n*-butyl acrylate) triblock copolymer synthesized by seeded emulsion polymerization initiated by the DIAMA-Na difunctional alkoxyamine (experiment 10).

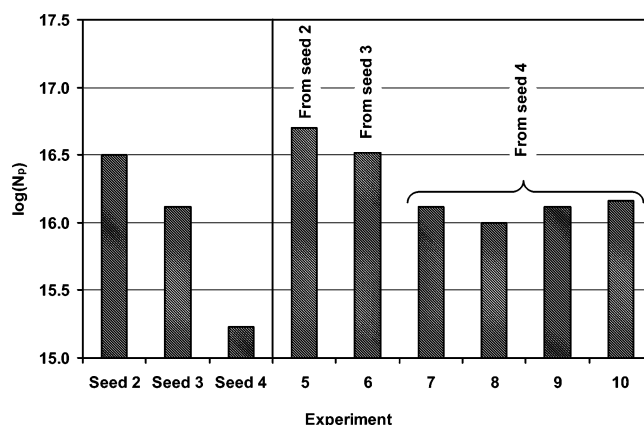


**Figure 12.** Particle numbers for all experiments.

**5. Discussion on the Particle Size and Particle Number.** Figure 12 illustrates the particle number for all experiments. It appears clearly that the final particle number strongly depends on the surfactant concentration in the seed latex, but not on the overall surfactant concentration in the second polymerization step. This is supported by experiments 5–7 with different seed latexes, but the same overall surfactant concentration. It is also supported by experiments 8 and 9 prepared from the same seed, but different overall surfactant concentrations. This finding would indicate that secondary nucleation did not take place in those multistep emulsion polymerizations, which is corroborated by the narrow particle size distributions shown in Table 2 and in Figure 8 and also by the absence of small particles on the TEM distributions (Figure 8). However, this is in contradiction with the large difference in  $N_p$  between the seeds and the latexes grown from them (compare experiment 5 with seed 2, experiment 6 with seed 3, and experiment 7 with seed 4). The possible explanation would be a low accuracy in the average diameters given by DLS for the seed particles, owing to their rather

broad particle size distribution (Table 2): the smallest particles (most probably mixed micellar aggregates formed by the association of surfactant molecules with oligomeric alkoxyamines) would not be counted, hence leading to an overestimated average diameter and underestimated  $N_p$ .

## Conclusion

We have synthesized a novel SG1-based water-soluble dialkoxyamine (DIAMA) by the addition of a high dissociation rate constant alkoxyamine (A-H) onto tri-(ethylene glycol) diacrylate. This dialkoxyamine was first successfully used for the bulk polymerizations of *n*-butyl acrylate and styrene. Then the sodium salt counterpart (DIAMA-Na) was used as a water-soluble initiator in the emulsion polymerizations of *n*-butyl acrylate and styrene via a multistep process. Very stable latexes were recovered, with the polymer exhibiting all the features of a controlled system. As compared with the monofunctional A-Na alkoxyamine under the same experimental conditions, the DIAMA-Na allows much smaller particles to be produced, thanks to its unique structure with two carboxylate salts. Under specific experimental conditions, the particle size distributions were also strongly improved and were quite narrow as proven by DLS and TEM. Synthesis of well-defined latexes with predictable average diameters and narrow particle size distribution are now conceivable in quite a simple polymerization process. As compared with the A-Na monofunctional alkoxyamine previously used in emulsion, this is a major improvement in the field. The emulsion process was also successfully applied to the synthesis of a polystyrene-*b*-poly(*n*-butyl acrylate)-*b*-polystyrene triblock copolymer. However, the polystyrene blocks were slightly polluted by residual *n*-butyl acrylate monomer units due to a purposely chosen incomplete first block conversion to minimize irreversible termination reactions. This work represents the first successful attempt of the synthesis of a complex architecture together with the control of average diameter and particle size distribution in NMP in emulsion, which is of high industrial and academic interest.

**Acknowledgment.** The authors thank Jean-Luc Couturier from Arkema for kindly providing the A-H alkoxyamine. J.N. also warmly thanks Pierre-Emmanuel Dufils and Laurence Petit for fruitful discussions.

## References and Notes

- (1) Solomon, D. H.; Rizzardo, E.; Cacioli, P. U.S. Patent 4,581,429, 1985.
- (2) Georges, M. K.; Veregin, R. P. N.; Kazmaier, P. M.; Hamer, G. K. *Macromolecules* **1993**, *26*, 2987–2988.
- (3) Hawker, C. J.; Bosman, A. W.; Harth, E. *Chem. Rev.* **2001**, *101*, 3661–3688.
- (4) Matyjaszewski, K.; Xia, J. *Chem. Rev.* **2001**, *101*, 2921–2990.
- (5) Kamigaito, M.; Ando, T.; Sawamoto, M. *Chem. Rev.* **2001**, *101*, 3689–3745.
- (6) Matyjaszewski, K.; Gaynor, S. G.; Wang, J.-S. *Macromolecules* **1995**, *28*, 2093–2095.
- (7) Gaynor, S. G.; Wang, J.-S.; Matyjaszewski, K. *Macromolecules* **1995**, *28*, 8051–8056.
- (8) Chong, Y. K.; Krstina, J.; Le, T. P. T.; Moad, G.; Postma, A.; Rizzardo, E.; Thang, S. H. *Macromolecules* **2003**, *36*, 2256–2272.
- (9) Chiefari, J.; Mayadunne, R. T. A.; Moad, C. L.; Moad, G.; Rizzardo, E.; Postma, A.; Skidmore, M. A.; Thang, S. H. *Macromolecules* **2003**, *36*, 2273–2283.
- (10) Charlot, D.; Corpart, P.; Adam, H.; Zard, S. Z.; Biadatti, T.; Bouhadir, G. *Macromol. Symp.* **2000**, *150*, 23–32.
- (11) Goto, A.; Kwak, Y.; Fukuda, T.; Yamago, S.; Lida, K.; Nakajima, M.; Yoshida, J.-I. *J. Am. Chem. Soc.* **2003**, *125*, 8720–8721.
- (12) *Controlled Radical Polymerization*; Matyjaszewski, K., Ed.; ACS Symp. Ser. **1998**, 685.
- (13) *Controlled/Living Radical Polymerization: Progress in ATRP, NMP, and RAFT*; Matyjaszewski, K., Ed.; ACS Symp. Ser. **2000**, 768.
- (14) *Advances in Controlled/Living Radical Polymerization*; Matyjaszewski, K., Ed.; ACS Symp. Ser. **2003**, 854.
- (15) Benoit, D.; Chaplinski, V.; Braslau, R.; Hawker, C. J. *J. Am. Chem. Soc.* **1999**, *121*, 3904–3920.
- (16) Grimaldi, S.; Finet, J. P.; Le Moigne, F.; Zeghdou, A.; Tordo, P.; Benoit, D.; Fontanille, M.; Gnanou, Y. *Macromolecules* **2000**, *33*, 1141–1147.
- (17) Benoit, D.; Grimaldi, S.; Robin, S.; Finet, J. P.; Tordo, P.; Gnanou, Y. *J. Am. Chem. Soc.* **2000**, *122*, 5929–5939.
- (18) Diaz, T.; Fischer, A.; Jonquieres, A.; Brembilla, A.; Lochon, P. *Macromolecules* **2003**, *36*, 2235–2241.
- (19) Schierholz, K.; Givhechi, M.; Fabre, P.; Nallet, F.; Papon, E.; Guerret, O.; Gnanou, Y. *Macromolecules* **2003**, *36*, 5995–5999.
- (20) Couvreur, L.; Lefay, C.; Belleney, J.; Charleux, B.; Guerret, O.; Magnet, S.; *Macromolecules* **2003**, *36*, 8260–8267.
- (21) Lefay, C.; Belleney, J.; Charleux, B.; Guerret, O.; Magnet, S. *Macromol. Rapid Commun.* **2004**, *25*, 1215–1220.
- (22) Lovell, P. A.; El-Aasser, M. S. *Emulsion Polymerization and Emulsion Polymer*; John Wiley & Sons: Chichester, England, 1997.
- (23) Gilbert, R. G. *Emulsion Polymerization. A Mechanistic Approach*; Academic Press: London, 1995.
- (24) Qiu, J.; Charleux, B.; Matyjaszewski, K. *Prog. Polym. Sci.* **2001**, *26*, 2083–2134.
- (25) Cunningham, M. F. *Prog. Polym. Sci.* **2002**, *27*, 1039–1067.
- (26) Charleux, B. *Advances in Controlled/Living Radical Polymerization*; Matyjaszewski, K., Ed.; ACS Symp. Ser. **2003**, 854, 438–451.
- (27) Cunningham, M. F. *C. R. Chimie* **2003**, *6*, 1351–1374.
- (28) Miller, C. M.; Sudol, E. D.; Silebi, C. A.; El-Aasser, M. S. *Macromolecules* **1995**, *28*, 2754–2764, 2765–2771, 2772–2780.
- (29) Landfester, K. *Macromol. Rapid Commun.* **2001**, *22*, 896–936.
- (30) Asua, J. M. *Prog. Polym. Sci.* **2002**, *27*, 1283–1346.
- (31) Erdem, B.; Sudol, E. D.; Dimonie, V. L.; El-Aasser, M. S. *J. Polym. Sci., Part A: Polym. Chem.* **2000**, *38*, 4431–4440.
- (32) Bechtold, N.; Tiarks, F.; Willert, M.; Landfester, M.; Antonietti, M. *Macromol. Symp.* **2000**, *151*, 549–555.
- (33) Tiarks, F.; Landfester, M.; Antonietti, M. *Macromol. Chem. Phys.* **2001**, *202*, 51–60.
- (34) Liu, X.; Guan, Y.; Ma, Z.; Liu, H. *Langmuir* **2004**, *20*, 10278–10282.
- (35) Takasu, M.; Shiroya, T.; Takeshita, K.; Sakamoto, M.; Kawaguchi, H. *Colloid Polym. Sci.* **2003**, *282*, 119–126.
- (36) Han, M.; Lee, E.; Kim, E. *Opt. Mater.* **2002**, *21*, 579–583.
- (37) Marestin, C.; Noël, C.; Guyot, A.; Claverie, J. *Macromolecules* **1998**, *31*, 4041–4044.
- (38) Cao, J.; He, J.; Li, C.; Yang, Y. *Polym. J.* **2001**, *33*, 75–80.
- (39) Lansalot, M.; Farcet, C.; Charleux, B.; Vairon, J. P.; Pirri, R.; Tordo, P. *Controlled/Living Radical Polymerization: Progress in ATRP, NMP, and RAFT*; Matyjaszewski, K., Ed.; ACS Symp. Ser. **2000**, 768, 138–151.
- (40) Szkurhan, A. R.; Georges, M. K. *Macromolecules* **2004**, *37*, 4776–4782.
- (41) Nicolas, J.; Charleux, B.; Guerret, O.; Magnet, S. *Angew. Chem., Int. Ed.* **2004**, *43*, 6186–6189.
- (42) Delaittre, G.; Nicolas, J.; Lefay, C.; Save, M.; Charleux, B. *Chem. Commun.* **2005**, 614–616.
- (43) The polystyrene calibration is appropriate for poly(*n*-butyl acrylate) samples as shown by the Mark–Houwink–Sakurada parameters: actually it leads to an error of about 3–5%, which is within the accepted range for SEC analysis. Indeed, the MHS parameters in THF at 30 °C are the following:  $K_{ps} = 11.4 \times 10^{-5} \text{ dL g}^{-1}$  and  $\alpha_{ps} = 0.716$  for polystyrene [see: Hutchinson, R. A.; Paquet, D. A., Jr.; McMinn, J. H.; Beuermann, S.; Fuller, R. E.; Jackson, C. *Dechema Monogr.* **1995**, *131*, 467–492];  $K_{PBA} = 12.2 \times 10^{-5} \text{ dL g}^{-1}$  and  $\alpha_{PBA} = 0.700$  for poly(*n*-butyl acrylate) [see: Beuermann, S.; Paquet, D. A., Jr.; McMinn, J. H.; Hutchinson, R. A. *Macromolecules* **1997**, *29*, 1918–1927].
- (44) Degoulet, C.; Perrinaud, R.; Adjari, A.; Prost, J.; Benoit, H.; Bourrel, M. *Macromolecules* **2001**, *34*, 2667–2672.

- (45) Couturier, J.-L.; Guerret, O.; Bertin, D.; Gigmes, D.; Marque, S.; Tordo, P.; Chauvin, F.; Dufils, P. E. WO 2004/014926.
- (46) Magnet, S.; Guerret, O.; Couturier, J.-L. Eur. Pat. Appl. EP 1 526 138, 2005.
- (47) Fischer, H. *Chem. Rev.* **2001**, *101*, 3581–3610.
- (48) The purified DIAMA has been analyzed by  $^{31}\text{P}$  NMR (Bruker Avance 300, 121.44 MHz) with diethyl phosphite as an internal reference ( $\delta$  7.1 ppm). No remaining peak of the starting A-H alkoxyamine ( $\delta$  27.1 ppm) was detected whereas one single sharp peak was observed at  $\delta$  23.8 ppm corresponding to the chemical shift of the phosphorous atoms in the DIAMA.
- (49) For  $\text{p}K_{\text{a}}$  determination, correspondence between aqueous and alcoholic acidic scales was performed as described in the following reference: Bates, R. B. *Determination of pH, Theory and Practice*; John Wiley & Sons: New York, 1964; Chapter 7.
- (50) Lacroix-Desmazes, P.; Lutz, J. F.; Chauvin, F.; Severac, R.; Boutevin, B. *Macromolecules* **2001**, *34*, 8866–8871.
- (51) Beuermann, S.; Paquet, D. A., Jr.; McMin, J. H.; Hutchinson, R. A. *Macromolecules* **1996**, *29*, 4206–4215.
- (52) Farcet, C.; Nicolas, J.; Charleux, B. *J. Polym. Sci., Part A: Polym. Chem.* **2002**, *40*, 4410–4420.
- (53) Buback, M.; Gilbert, R. G.; Hutchinson, R. A.; Klumperman, B.; Kuchta, F.-D.; Manders, B. G.; O'Driscoll, F. K.; Russel, R. T.; Schweer, J. *Macromol. Chem. Phys.* **1995**, *196*, 3267–3280.
- (54) Nicolas, J.; Charleux, B.; Guerret, O.; Magnet, S. *Macromolecules* **2004**, *37*, 4453–4463.
- (55) Charleux, B. *Macromolecules* **2000**, *33*, 5358–5365.
- (56) Farcet, C.; Belleney, J.; Charleux, B.; Pirri, R. *Macromolecules* **2002**, *35*, 4912–4918.

MA0511999